Charge-Transfer Controlled Exchange Interaction in Radical-Triplet Encounter Pairs as Studied by FT-EPR Spectroscopy

Akio Kawai* and Kazuhiko Shibuya

Department of Chemistry, Graduate School of Science and Engineering, Tokyo Institute of Technology, 2-12-1 Ohokayama, Meguro-ku, Tokyo 152-8551, Japan

Received: November 22, 2006; In Final Form: March 19, 2007

The exchange interaction, *J*, producing quartet and doublet energy separation in radical-triplet excited molecule encounter pairs, was investigated in solution by measuring chemically induced dynamic electron polarization (CIDEP) created through the radical-triplet pair mechanism. A time-resolved FT-EPR method was utilized to measure CIDEP of galvinoxyl radical by recording FID signals and an absolute magnitude of CIDEP, P_n, was determined for each radical-triplet system by detailed analysis of the time evolution curves of CIDEP. A transient FT-EPR signal phase remarkably depends on the triplet molecule. The signal phase is related to the sign of *J* value, which is responsible for the radical-triplet pair interaction. Most of galvinoxyl-triplet systems showed normal negative sign. An unusual positive sign was found in some systems characterized by a small energy gap, ΔG, between the radical-triplet pair and intermolecular charge transfer (CT) states. A theoretical calculation of *J* value for radical-triplet encounter pairs was carried out by considering exchange integral and intermolecular CT interaction. According to the calculated *J* value and the diffusion theory for CIDEP magnitude, experimental P_n values were theoretically reproduced as a function of ΔG. The present results confirm our previously reported CT model explaining the complicated nature of the sign of *J* value in the galvinoxyl-triplet encounter pairs. According to the proposed model for CT effect on *J* value and CIDEP results, nature of *J* value in radical-triplet pairs is discussed.

Introduction

Exchange interaction in the pairs of paramagnetic molecules in solution is related to the energy splitting of degenerate spin states such as triplet−singlet splitting in radical pairs and quartet (Q)−doublet (D) splitting in radical-triplet (RT) pairs. This interaction is significantly important when we study chemical reaction dynamics in bond formation or cleavage, electron-transfer and hydrogen atom transfer reactions, and so on.[1] So far, quenching dynamics of the excited states by free radicals,[2−7] covalently linked RT complexes,[8,9] excited triplet porphyrins with paramagnetic metal ions,[10] and reaction dynamics of the radical−biradical systems[11] have been understood on the basis of spin dynamics with intermolecular potentials characterized by Q−D separation due to exchange interaction. Although importance of exchange interaction is quite high, a direct measurement of intermolecular potentials of degenerate spin states produced by exchange interaction is difficult as far as two molecules of the pair are freely diffusing. There are indirect methods to investigate exchange interaction using spin coherent effects on chemical reactions[1] such as magnetic-field-dependent chemical reaction yields and chemically induced dynamic electron polarization (CIDEP) of free radicals that depend on spin state mixings on the potential surfaces created by the exchange interaction. As for the latter, it is fortunate that spin−lattice relaxation times of organic free radicals are usually on the order of microseconds,[12] which makes it easy to measure CIDEP by a time-resolved (TR-) EPR method. Because CIDEP enhances EPR detection sensitivity, EPR spectroscopy of photochemical intermediate free radicals and radical pairs are possible as far as CIDEP is created on these species. Moreover, CIDEP is created through spin dynamic interactions in $S-T_{-1}$ and $S-T_0$ mixings in radical pairs and is valuable for understanding of the intermolecular exchange interaction once a time-dependent CIDEP creation mechanism is well analyzed.

Although CIDEP is valuable for understanding of the exchange interaction, an analysis of CIDEP in radical pair systems is not straightforward because a time profile of TR-EPR signal depends both on the absolute magnitude of CIDEP and radical concentration, which requires complicated analysis of CIDEP. On the other hand, an analysis of CIDEP in the excited-state quenching process by stable free radicals is promising because the concentration of free radical is constant and only decay kinetics of the triplet state should be considered.[5] It has been already known that strong CIDEP is created during the S_1 and T_1 quenching by free radicals, and the phenomena is well understood in terms of the radical-triplet pair mechanism (RTPM).[5] There are already many papers studying spin dynamics of RT pairs by quantitative CIDEP analysis[13−21] and exchange interaction in the RT pairs has been discussed. In these studies, Heisenberg spin exchange expressed by

$$\hat{H}_{sp\cdot ex} = -\frac{1}{3}J(1 + 4\hat{S}_T\cdot\hat{S}_R)$$

is used to describe the energy difference between D and Q states, $-2J = E_Q - E_D$. In usual RT pairs, overlap integral of the pair is negligibly small and *J* is thus in proportion to exchange integral, J_{ex}, of Q and D states. One of the most important conclusions of previous works is that most RT pairs show antiferromagnetic interaction in which the Q state is higher in energy than the D state ($J < 0$).[5−7] This general trend is similar

* Corresponding author. E-mail: akawai@chem.titech.ac.jp. Telephone: +81-3-5734-3847. Fax: +81-3-5734-2231.

10.1021/jp067753d CCC: $37.00
Published on Web 05/23/2007

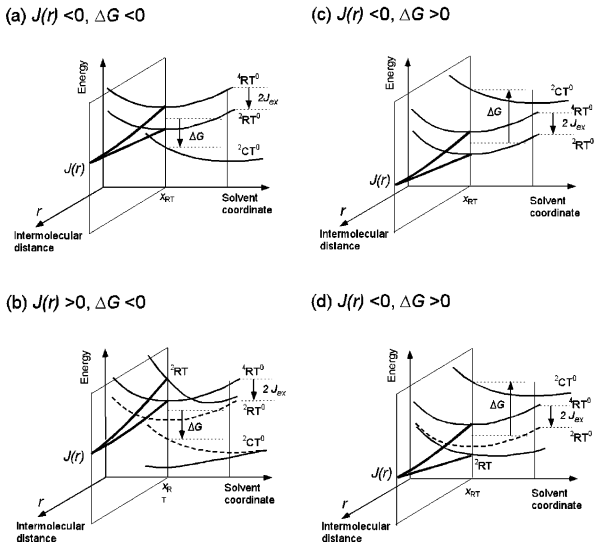

Figure 1. Schematic explanation of the previously reported mechanism for quartet-doublet energy splitting, $J(r)$, in the radical-triplet encounter pair. $J(r)$ corresponds to the energy difference between ^{2}RT and $^4RT^0$ states in this model. Splitting between zero-order states of $^2RT^0$ and $^4RT^0$ is due to exchange integral. Sign and magnitude of $J(r)$ depend both on ΔG ($= E(CT^0) - E(RT^0)$) and CT interaction, H_{CT} between CT and RT pair states. (a) $\Delta G < 0$ and weak H_{CT}, giving $J(r) < 0$, (b) $\Delta G < 0$, and strong H_{CT} giving unusual $J(r) > 0$, (c) $\Delta G > 0$ and weak H_{CT}, giving $J(r) < 0$, and (d) $\Delta G > 0$ and strong H_{CT} giving $J(r) < 0$. Exponentially decaying $J(r)$ along the intermolecular distance, r, is assumed, and the gray and black solid lines are the doublet and the quartet states, respectively. The x_{RT} represents the minimum energy point of radical-triplet encounter pair along the solvent coordinate.

to that in radical pairs which shows antiferromagnetic interaction, namely, a singlet pair is lower in energy than triplet pair as explained in the Heitler−London model for a chemical bond. However, the magnitude of J_0, which is J value at the closest approach of the pair, is significantly small in RT pairs and estimated to be on the order of 0.1 cm^{-1}.[13,14] This is reasonable because the RT systems so far studied by CIDEP are the pairs of a triplet and a chemically stable free radical in which no significant bond formation is expected.

When J value due to J_{ex} is small, intermolecular charge transfer (CT) interaction becomes important for certain systems such as radical ion pairs, and a sign of J value changes to be positive.[22−24] While most of RT pairs show antiferromagnetic coupling ($J < 0$), unusual ferromagnetic interactions ($J > 0$) in RT pairs were also found in several galvinoxyl(Galv)/ triplet systems[25,26] and in a 1-diphenyl-2-picrylhydrazyl/triplet coronene system[27] according to CIDEP analysis. This means that J_{ex} is not the only interaction factor to determine positive or negative J value in RT pairs. There exists another factor, which is more than or comparable to exchange integral J_{ex}. The mechanism of intermolecular CT type exchange interaction for RT pairs has been proposed to explain this unusual ferromagnetic interaction,[25−27] which is schematically described in Figure 1. Because J value depends on RT distance, r, we denoted J as $J(r)$. In general, the RT pair states split into zero-order Q and D ($^4RT^0$ and $^2RT^0$, respectively) states with negative J_{ex} value. A positive J value is caused by configuration interaction between RT and CT pair states. When the zero-order CT pair state ($^2CT^0$) is lower in energy than RT pair state and the intermolecular CT interaction is large (Figure 1b), energy-shift of $^2RT^0$ caused by the CT interaction with $^2CT^0$ becomes dominant in the energy splitting and an unusual positive sign of J will be observed. When the CT state is higher in energy than the RT pair states, neither strong (Figure 1c) nor weak (Figure 1d) CT interaction result in positive J value.

In this study, we continued further detailed analysis of CIDEP created by the RTPM in Galv/triplet pairs by using a Fourier transform (FT-) EPR method to determine the absolute magnitude of CIDEP named P_n value and sign of J_0 value. In our model to understand J_0 value in RT pairs, we consider both exchange integral creating negative J_0 value and intermolecular CT interaction creating either positive or negative J_0 value depending on the relation of $^2CT^0$ and $^{2,4}RT^0$ energies. According to the diffusion theory for CIDEP magnitude created by the RTPM,[19,20] CIDEP is controlled by absolute magnitude of J_0 value and the potential curvature of Heisenberg spin exchange interaction, $J(r)$. Therefore, analysis of observed CIDEP magnitude based on the theory enables us to estimate an absolute magnitude of J_0 value. We discuss the mechanism determining J_0 value in RT pairs on the basis of CIDEP analysis.

Experimental

Time-resolved FT-EPR measurements combined with UV laser excitation were carried out by a conventional X-band FT-EPR spectrometer (Bruker, ELEXIS 580E). The FT-EPR spectra of Galv were obtained by Fourier transformation of FID generated by a $\pi/2$ pulsed microwave irradiation of Galv with 12 ns time width, which is wide enough to excite all hyperfine lines. FID was obtained by a phase cycling routine. A dielectric cavity with an optical window for laser irradiation was used for FT-EPR measurements.

In both FT-EPR and transient absorption measurements, UV excitation at 355 and 282 nm were carried out by the third harmonics of a YAG laser (Continuum, Powerlight 8000) and by the frequency doubling (Inrad, R-6G crystal) of a dye laser output (Lambda Physik, Scanmate) pumped by the second harmonics of the YAG laser, respectively. The irradiated laser power was attenuated to be about 0.2 mJ/pulse for 282 nm and 1−10 mJ/pulse for 355 nm. The concentrations of excited molecules were adjusted to suppress the occurrence of a triplet−triplet annihilation process as described in the Results and Discussion section. The repetition rates of lasers were 10 Hz for FT-EPR and 1 Hz for transient absorption measurements. The excitation laser covers all the area of the dielectric cavity where FT-EPR sensitivity is high. Details of lasers, a cell, and a microwave cavity are described in the Supporting Information.

All of the chemicals (Tokyo Kasei) were used as received. The concentrations of Galv was ca. 0.1−0.2 mM (M = mol dm^{-3}) for FT-EPR measurements. Sample solutions were degassed by bubbling Ar gas and were flowed through (1) a quartz cell (0.3 mm diameter) equipped in the dielectric cavity for the FT-EPR measurements and (2) a quartz rectangular cell with optical path lengths of 5 mm for excitation laser and 10 mm for monitor lights, respectively, for the transient absorption measurements. Optical densities of sample solution were determined by the UV−vis spectrometer (Shimadzu UV2200). All the measurements were carried out at room temperature (298 K).

Results and Discussion

FT-EPR Measurements for CIDEP in Galv/Triplet Pairs. Figure 2 shows FT-EPR spectra of Galv recorded for a Galv/9-fluorenone (9-FL) mixture system in benzene before (0 μs) and after (2 μs) laser excitation at 298 K. At 0 μs, Galv is populated in the thermal state distribution and thus the intensity reflects the thermal spin magnetization of Galv. The intensity of Galv recorded after the laser excitation decreased. This signal

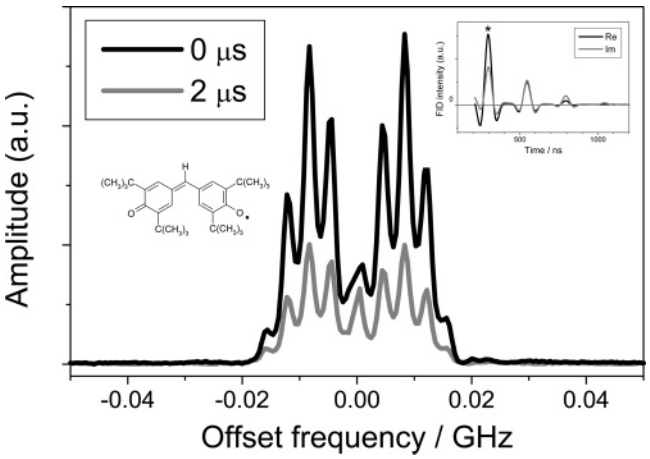

Figure 2. FT-EPR spectra of Galv in a 9-fluorenone (5.3 mM)/Galv-(0.2 mM) mixture in benzene derived by Fourier transformation of FID signal of Galv obtained by $\pi/2$ pulsed microwave irradiations before and 2.0 μs after the 355 nm laser excitation of 9-fluorenone. Inset: FID time profile of Galv in benzene obtained by a $\pi/2$ pulsed microwave irradiation with 12 ns time width. Magnetic field was set around the *g*-center of Galv.

reduction was observed transiently and the original thermal signal recovered at much later time delay. The intensity of FT-EPR signal is in proportion to the electron spin magnetization of Galv. The transient reduction of FT-EPR signal after the laser excitation is due to creation of emission (Em) phase CIDEP of α-spin enhanced population according to the previous time-resolved EPR studies on the Galv/9-FL system.[25] The 355 nm laser excitation generates triplet 9-FL (^{3}9FL*) and CIDEP is created by the encounter between Galv and ^{3}9FL* through the RTPM. After all ^{3}9FL* is quenched by Galv, no CIDEP is created and the FT-EPR signal again reflects original thermal magnetization. This point will be examined later in detail.

Figure 3 shows the difference FT-EPR spectra of Galv measured in various Galv/triplet systems before and after laser excitation. These difference spectra show clear hyperfine structure of Galv and indicate that CIDEP is created on Galv. The CIDEP phase depends on the system: Net emission type CIDEP (net Em) is created in the cases of 9-FL and benzil, while net enhanced absorption (net Abs) type is created in the cases of triphenylene and coronene. This observation of CIDEP phase accords with the previous TR-EPR study on CIDEP of Galv/triplet systems.[25] According to the RTPM, sign of *J* value in these systems were determined as positive for triphenylene and coronene, and as negative for 9FL and benzil.[27] Figure 4a shows difference FT-EPR spectra recorded for Galv in Galv/benzil mixture in benzene at several different time delays. In this system, net Em type CIDEP intensity becomes the largest at 2.0 μs and then decreases as time passes. At 20 μs, CIDEP component of Galv disappears. Because no CIDEP component of radicals other than Galv was observed, we confirmed that

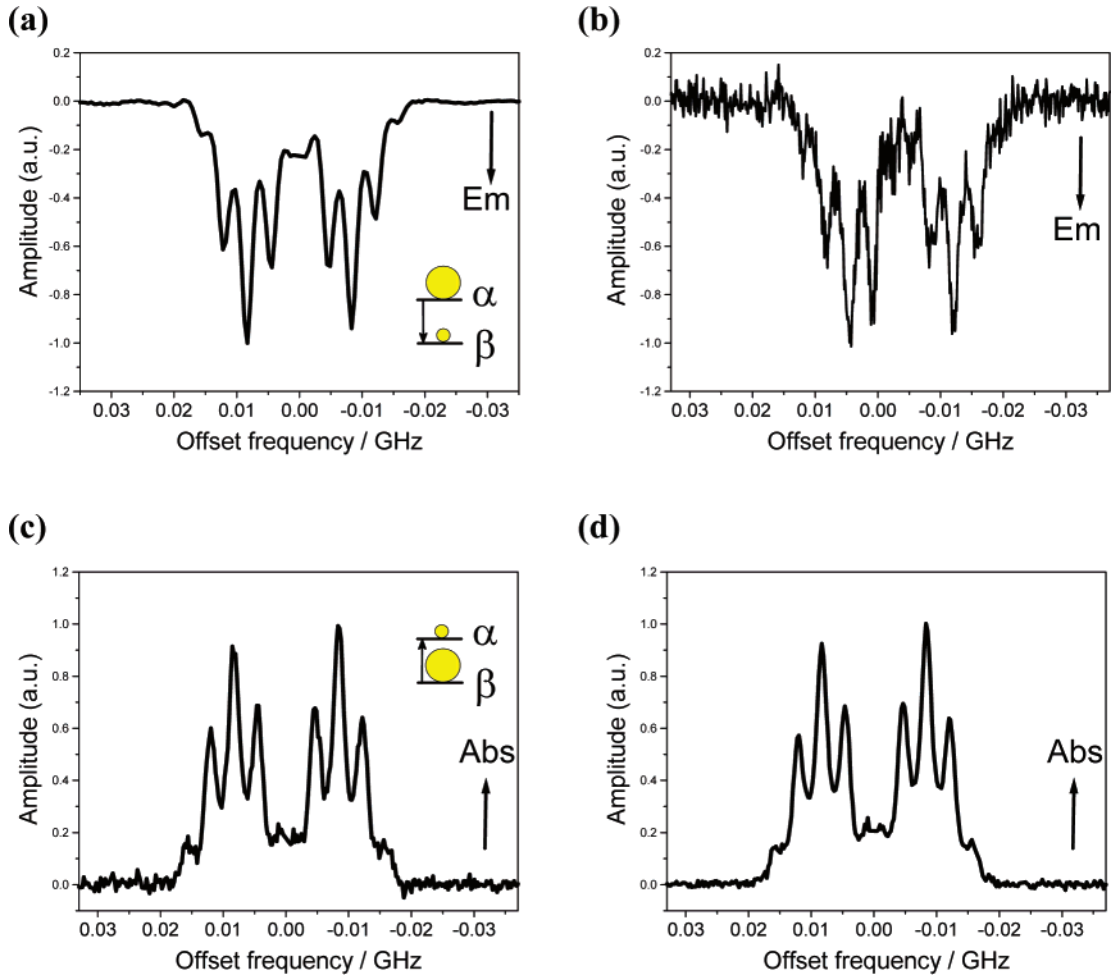

Figure 3. Transient FT-EPR difference spectra of Galv obtained by substraction of FT-EPR spectra derived by FID signals before and 2.0 μs after laser excitation. Samples include (a) 9-fluorenone (5.3 mM), (b) benzil (6.9 mM), (c) triphenylene (0.08 mM), and (d) coronene (0.67 mM) in benzene. The concentrations of Galv were 0.21 mM except (c) 0.13 mM. Dissolved oxygen molecules were removed by Ar bubbling. Laser wavelengths: (a,b,d) 355 nm, (c) 282 nm.

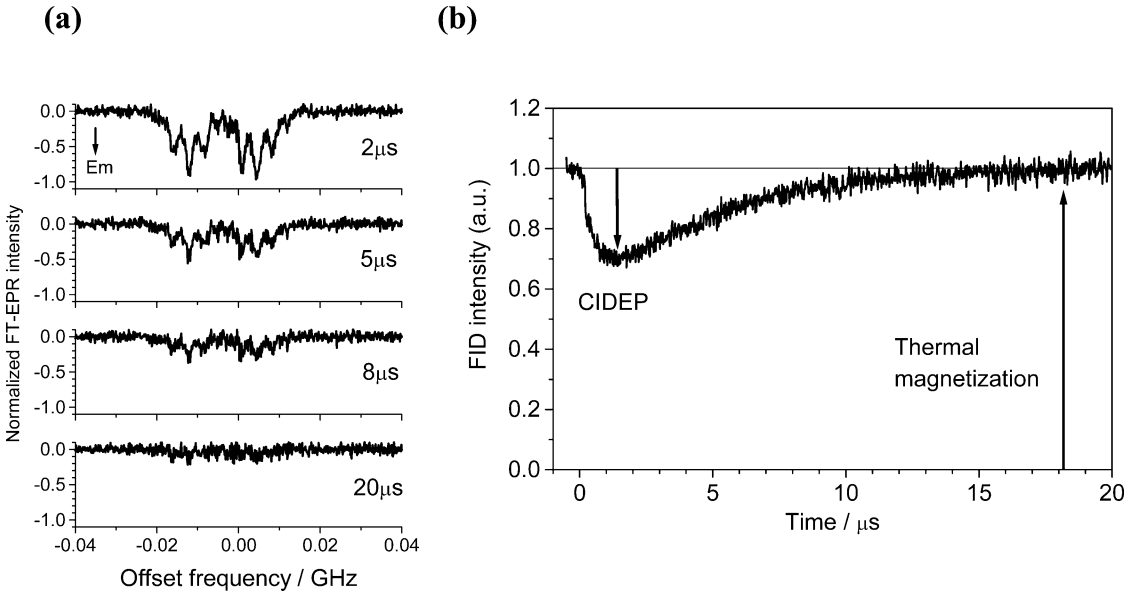

Figure 4. (a) Transient FT-EPR difference spectra of Galv derived by FID at various delay times after 355 nm laser excitation in benzil (6.9 mM)/Galv(0.14 mM) mixture in benzene. (b) Time-evolution curve of FID intensity as a function of delay time between laser and $\pi/2$ pulses. FID intensity was monitored at the peak marked by an asterisk in Figure 2 inset. Signal intensity was normalized by the intensity at thermal equilibrium of Galv. Reduction of FID signal observed at 0−15 μs is due to Em phase CIDEP of Galv created by the RTPM.

there is no photochemical generation of other radicals. This indicates that the FID signal at any time window is entirely due to Galv. Therefore, to obtain time evolution curves of Galv signal, we monitored FID intensity marked by an asterisk in FID profile shown in the inset of Figure 2 as a function of time delay between a laser and $\pi/2$ pulses. A time-evolution curve measured was shown in Figure 4b. In this profile, intensity is normalized by the FID signal intensity of the thermal magnetization measured before laser excitation. As clearly seen in the time-evolution curve, FID signal decreases after laser excitation and then thermal magnetization signal appears again at 20 μs. The similar time-evolution curves were measured for other Galv/triplet systems, and only simple rise and decay of CIDEP in either Em or Abs phases were observed.

In Galv/triplet systems, we consider the reaction scheme as follows.

$$S_0 + h\nu \rightarrow S_1 \quad (1)$$

$$S_1 \xrightarrow{\text{IC, fluorescence}} S_0 \quad (2)$$

$$\xrightarrow{\text{ISC}} T_1 \quad (3)$$

$$T_1 + \text{Galv} \xrightarrow{k_q} {}^2(T_1\cdots\text{Galv}) \rightarrow {}^2(S_0\cdots\text{Galv}) \rightarrow S_0 + \text{Galv} \quad (4)$$

$$\rightarrow {}^4(T_1\cdots\text{Galv}) \rightarrow T_1 + \text{Galv}^* \quad (5)$$

$$T_1 \xrightarrow{k_T} S_0 \quad (6)$$

$$T_1 + T_1 \xrightarrow{k_{TT}} 2S_0 \text{ or } S_0 + S_1 \quad (7)$$

The k_q and k_{TT} are the rate constants for quenching of triplet molecule by Galv and triplet−triplet annihilation, respectively. The k_T is a unimolecular triplet decay rate in the absence of quencher. Galv* denotes a Galv radical that is involved in the triplet quenching and possesses a certain amount of CIDEP with either of Em or Abs phase by the RTPM. Spin-polarized Galv* disappears to give Galv without CIDEP with a rate of spin−lattice relaxation. As triplet concentration decreases, Galv* concentration becomes low and the FID intensity approaches to the intensity of thermal magnetization as observed in the later time region.

One of advantageous points of FT-EPR spectrometry is that there is no continuous microwave perturbation on the dynamics of spin magnetization of radicals.[16,17] Therefore, the time-evolution of CIDEP is more correctly measured by the FT-EPR method than by the continuous-microwave TR-EPR method. This enables us to simulate the time evolution curve with very simple Bloch equation with chemical kinetics. Another advantageous point is that the thermal magnetization signal of Galv, which is easily measured, can be used as a standard of FID signal intensity. This standard signal is very important when we need to determine an absolute magnitude of CIDEP created in the photosystem of interest. To ensure that these CIDEP signals were due to the RTPM and to determine a magnitude of CIDEP created at each triplet quenching event, the time evolutions were simulated by the following Bloch (eq 8) and kinetic (eq 9) equations for FT-EPR measurements.[13,14,28]

$$\frac{dM_z}{dt} = -\frac{(M_z - P_{eq}[\text{Galv}])}{T_1{}^R} + P_n k_q[\text{Galv}][\text{triplet}] \quad (8)$$

$$\frac{d[\text{triplet}]}{dt} = k_f[S_1] - (k_T + k_q[\text{Galv}] + k_{TT}[\text{triplet}])[\text{triplet}] \quad (9)$$

where M_z represents the magnetization of z axis in the rotating frame, and $T_1{}^R$ is the spin−lattice relaxation time of Galv. Equation 8 contains terms due to the relaxation toward the thermal magnetization, P_{eq}[Galv], and CIDEP, P_n, created by the RTPM. As mentioned above, the signal by the thermal magnetization, P_{eq}[Galv] was normalized to a unity. The $T_1{}^R$ value of about 3.0 μs in benzene was determined by a conventional method of inversion recovery for FID.[29] The k_f is the fluorescence decay rate, which equals the rate of triplet generation. The k_T for our sample systems and the k_q are unknown, and we determined these kinetic parameters by a conventional transient absorption method. The triplet−triplet absorption was monitored in the presence of Galv, and the

TABLE 1: Triplet Quenching Rate Constants (k_q) by Galvinoxyl Radical, Unimolecular Triplet Decay Rates (k_T), the Absolute Magnitudes of CIDEP (P_n), and Energy Gaps, ΔG, between the RT Pair and CT States in Benzene at 298 K

triplet molecule	$k_q/10^9$ M^{-1} s^{-1}	$k_T/10^5$ s^{-1}	P_n/P_{eq}[a]	ΔG[b]/kJ mol^{-1}
tetracene	2.9 ± 0.1	0.8	−7	+45.5
anthracene	4.2 ± 0.8	3.5	−5	+25.2
pyrene	4.7 ± 0.3	2.5	−2	+15.7
naphthalene	6.2 ± 0.5	1.5	+1	+1.1
chrysene	4.6 ± 0.3	2.2	+2	−4.1
coronene	5.4 ± 0.6	1.9	+8	−12.2
tetraphenylporphin			0∼−2.0[c]	−17.9
triphenylene	7.1 ± 0.4	2.1	+10	−25.2
quinoxaline	5.3 ± 0.6	3.2	+2	−34.8
fluoranthene	4.9 ± 0.4	0.7	−2	−37.8
phenazine	1.8 ± 0.1	1.3	−7	−51.4
9-fluorenone	2.7 ± 0.3	1.1	−9	−70.6
benzophenone	3.9 ± 0.4	2.1	−3	−94.8
benzil	1.3 ± 0.1	0.8	−15	−139.3

[a] Error bars of ca. ±20% due to both the experiment and simulation are estimated. [b] Calculated by eqs 10 and 11 for $\Delta G(r)$ at $r = 0.7$ nm. Error bar of ca. 10 kJ mol^{-1} is expected due to λ_v value estimation procedure. [c] The P_n/P_{eq} value is estimated from ref 17.

Stern−Volmer analysis of triplet decay rate was performed. The results are summarized in Table 1. In all systems examined, the k_q values are on the order of 10^9 M^{-1} s^{-1}, which is close to the diffusion rate constant of 1.0×10^{10} M^{-1} s^{-1} in benzene.[30] The lowest doublet excited state (D_1) energy of Galv[3] is 11 000 cm^{-1}, which is lower than the triplet energies of all the molecules examined. In the radical-triplet system where D_1 energy is lower than the T_1 energy, triplet quenching through exchange mechanism is quite efficient, and it is reasonable that the measured k_q value is close to the diffusion rate constant.[2] The k_{TT} value is assumed to be 10^{10} M^{-1} s^{-1} because the triplet−triplet annihilation occurs at a diffusion controlled rate.[31] To evaluate annihilation rates, it is important to know the triplet concentration. In the present experiment (see Supporting Information), the sample flowed in a cylindrical tube and the laser beam was perpendicular to the cell tube. Under these conditions, the optical path length ranged from 0 to 3 mm, and the optical density was on the order of 0.1 per 10 mm. Therefore, the light intensity depended on the position in the cell. To estimate triplet concentration in the sample cell, we calculated representative light intensity for typical sample solution with a certain laser power. The triplet concentrations were thus estimated to be on the order of 10^{-5} M using reported Φ_T values.[30,32] If the triplet−triplet annihilation is the dominant triplet deactivation process, the triplet decay rate should show square dependence on the triplet concentration and depends on the position in the cell. If that is the case, the triplet kinetics depends on the position in the cell and one cannot use a mean light intensity to estimate triplet concentration for determination of P_n value. The annihilation rate constant is 10^{10} M^{-1} s^{-1}, and the triplet decay rate constants of k_q and k_T are listed in Table 1. Hence, typical triplet concentration of 10^{-5} M gives the initial annihilation rate of 10^5 s^{-1}, which is comparable to or slower than the unimolecular triplet decay rates. Under low concentrations of triplet molecules, the contribution of annihilation to total decay rate becomes smaller, especially in the later time region as the triplet concentration decreases. The triplet disappears within 2 μs, and the triplet molecules deactivated by the annihilation in this time window are typically about 10−20% of the total number of triplet molecules. This condition for the triplet concentration is comparable to those in the previous study.[17a] When we use even lower laser power, these numbers decrease, for example, 1% for Galv/triphenylene under low laser power excitation (0.83 mJ). Therefore, under our experimental conditions, we can neglect the contribution of the triplet−triplet annihilation and mean light intensities, namely, mean initial triplet concentrations can be used for estimation of triplet time evolution.

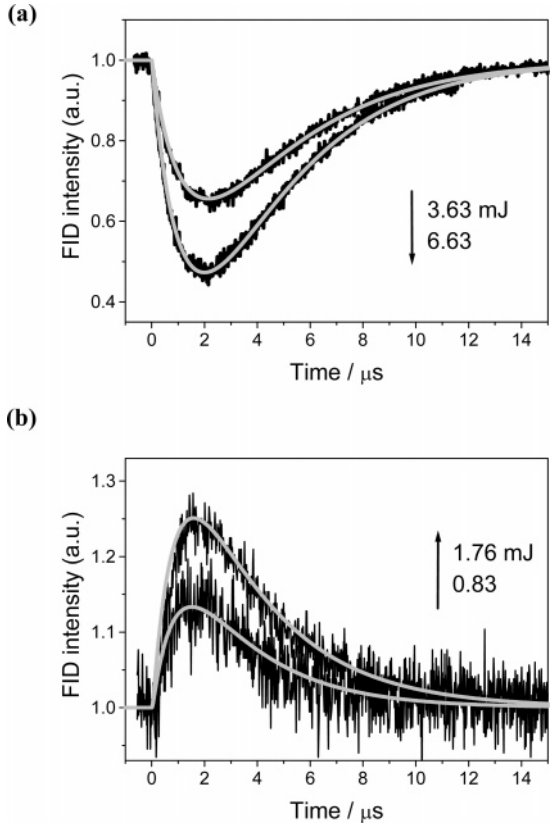

Figure 5. Normalized time-evolution curves of FID intensity as a function of delay time between laser and $\pi/2$ pulses. FID intensity was monitored at the peak marked by an asterisk in Figure 2 inset. Samples are (a) 9-fluorenone (5.3 mM) and (b) triphenylene (0.08 mM) in benzene. Simulations were made by using Bloch and the kinetic equations described in the text. The excitation laser powers were noted in each Figure.

According to these kinetic parameters and the modified Bloch equation, we have simulated the time evolution curves. Examples of the simulation were shown in Figure 5. The time evolution curves were well reproduced by the present model of the RTPM for CIDEP creation. From the best fitting simulations, P_n values were determined in the unit of P_{eq} for each time-evolution curve. To determine an accurate value of P_n for the Galv/triplet pair, measurements and simulations were carried out for various laser powers, giving different triplet concentrations. The P_n values were determined by averaging individual P_n values for each data set, which are summarized in Table 1. It is noteworthy that the times of initial reduction and recovery to the thermal magnetization do not depend on the laser power as shown in Figure 5, although higher triplet concentration due to higher laser power is expected to result in a greater contribution of the annihilation process. This observation implies that the annihilation process is not important in the present system, and the time profiles shown in Figure 5 can be analyzed with mean values of light intensity. On the other hand, a change in the radical concentration significantly affects the time evolution curves as shown in Figure 6, where the time evolution of M_z magnetization in the Galv in Galv/benzil system was monitored by FID signals after the 355 nm laser excitation. The triplet decay profile changes with the radical concentration and the initial reduction profile changes accordingly. The recovery

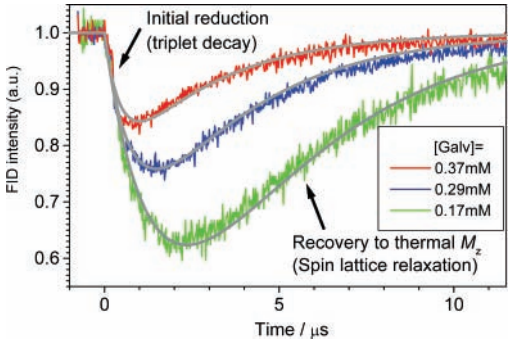

Figure 6. Normalized time-evolution curves of FID intensity of Galv as a function of delay time between laser and $\pi/2$ pulses under 355 nm laser excitation in benzil (6.5 mM)/Galv mixture in benzene. The concentrations of Galv are denoted in the figure. The FID intensities were monitored at the peak marked by an asterisk in the inset of Figure 2. Signal intensities are normalized by the thermal equilibrium intensity of Galv. Solid lines are simulation curves.

profile is essentially controlled by the spin−lattice relaxation of Galv and does not change, as seen in Figure 6.

Evaluation of P_n Values in Galv/Triplet Systems. The P_n value measured ranges from −15 to +10 P_{eq} depending on the triplet molecule. The phase of CIDEP is a fingerprint of the sign of exchange interaction of RT pairs: negative and positive P_n values are, respectively, related to the antiferro- ($J < 0$) and ferromagnetic ($J > 0$) interaction.[27] To examine an effect of CT interaction on the P_n values, we have estimated the energy difference, $\Delta G(r)$, between $^{2,4}RT^0$ without J_{ex} and $^2CT^0$ as a function of intermolecular distance, r, by the following equation.

$$\Delta G(r) = \Delta E(r) + \lambda_s(r) + \lambda_v \qquad (10)$$

$\lambda_s(r)$ is a solvent reorganization energy between the RT and the CT states and was calculated to be 1.32 kJ mol^{-1} by assuming Marcus' formula of $\lambda_s(r)$[33] with an ion radius of $r_{Acc} = r_{Dnr} = 0.35$ nm, where Acc and Dnr denote charge acceptor and donor, respectively, and with $n = 1.501$ and $\epsilon = 2.284$ for benzene. As for CT state, we consider that triplet and Galv molecules are acceptor and donor, respectively, otherwise CT state energy is much higher than the T_1 energy. λ_v is a sum of vibrational reorganization energies of donor and acceptor molecules. According to the previous studies on CT reactions, λ_v of 24.0 kJ mol^{-1} was a typical value for various donor−acceptor pairs of aromatic compounds with a few benzene rings.[34] Therefore, we adopted $\lambda_v = 24.0$ kJ mol^{-1} for the energy calculation. $\Delta E(r)$ is an energy gap between the potential minimum energies of $^2CT^0$ and $^{2,4}RT^0$ without J_{ex} along solvent and intramolecular nuclear coordinates. The $\Delta E(r)$ value is expressed by

$$\Delta E(r) = \{E_{1/2}{}^{ox}(\text{Galv}) - E_{1/2}{}^{red}(T_1) + \Delta E_{corr}\} - E_{coulomb}(r) - \Delta E(T_1) \qquad (11)$$

$E_{1/2}{}^{ox}$(Galv) and $E_{1/2}{}^{red}(T_1)$ are half-wave redox potentials of Galv (+0.07 V) in acetonitrile (AcCN)[35] and triplet molecule[25−27] with respect to standard calomel electrodes, respectively. Because redox potentials were obtained in highly polar solvents ($\epsilon > 30$), an additional correction term, ΔE_{corr} of 67.4 kJ mol^{-1} reported previously for cyclohexane (CyH) solution,[36] was added to obtain the $\Delta E(r)$ value in nonpolar solvent. $E_{coulomb}(r)$ is the Coulomb energy of the $^2CT^0$ state. The $\Delta E(T_1)$ values were obtained by reference to the literature.[30,32] ΔG values at $r = 0.7$ nm, which is assumed to be the intermolecular distance at the closest approach of the pair, are summarized in Table 1.

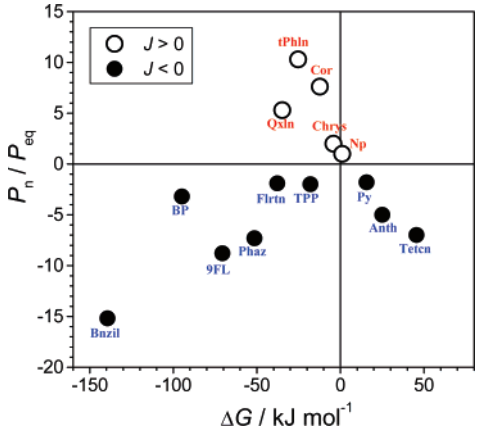

Figure 7. Plot of P_n/P_{eq} value against ΔG calculated by eq 11 and 12 for $\Delta G(r)$ at $r = 0.7$ nm in various Galv/triplet systems in benzene. P_n values were determined by the fitting of time-evolution curves of FID for CIDEP developments. Abbreviates are Bnzil: benzil; BP: benzophenone; 9FL: 9-fluorenone; Phaz: phenazine; Flrtn: fluoranthene; Qxln: quinoxaline; tPhln: triphenylene; TPP: tetraphenylporphine; Cor: coronene; Chrys: chrysene; Np: naphthalene; Py: pyrene; Anth: anthracene; Tetcn: tetracene.

Figure 7 shows plots of P_n as a function of $\Delta G(r)$ at $r = 0.7$ nm. In the plot, a positive and a negative sign of P_n values are described by open and closed circles, respectively. One of prominent features is that the positive sign appears in the limited region of $\Delta G = -40$ to 0 kJ mol^{-1}. In the region of $\Delta G < -50$ and > 0 kJ mol^{-1}, P_n is positive and the magnitudes are −3 to −15 P_{eq}. This seems to suggest that the effect of CT state on P_n value is large in the systems of relatively small and negative ΔG value of −40 to 0 kJ mol^{-1}. In this region, negative value of J mainly due to exchange integral may turn out to be positive due to strong CT effect. As J value becomes positive, P_n value also becomes positive according to CIDEP sign rule in the RTPM. As described in Figure 1, the sign of J value, which is generally negative for the encounter pairs of paramagnetic species, will change to be positive when the intermolecular CT interaction largely contributes to the exchange interaction.[25−27] The present results accord with these studies. It should be mentioned that P_n value is negative for the $\Delta G \approx 0$ region with positive sign. In this region, CT effect is also large, but it enhances the magnitude of J value in negative sign as described in Figure 1d.

Theoretical Calculation of J Value Produced by Intermolecular CT Interaction. According to the quantitative theory of the RTPM for CIDEP,[19,20] $|P_n|$ value relates to the absolute magnitude of exchange interaction, J_0, at the closest approach of the encounter pairs. Therefore, analysis of $|P_n|$ values as well as their sign may assist understanding the complicated nature of exchange interction in Galv/triplet systems.

To calculate the ΔG dependent J value of RT pairs, both CT interaction and exchange integral J_{ex} are considered. A nearby electronic state of Galv/triplet pair is $^2CT^0$ state as discussed above and thus energy-shift due to intermolecular CT interaction between $^2CT^0$ and $^2RT^0$ of the same spin multiplicity are important. The $^4CT^0$ is a two-electron excited state and is much higher in energy than the $^2CT^0$ state. Therefore, the energy shift of $^4RT^0$ by $^4CT^0$ is negligible, and we consider only the contribution from the $^2CT^0$ state. Another contribution to the energy shift of RT states is produced by exchange integral of $^2RT^0$ and $^4RT^0$ states, which shows negative J value in general.[5] Therefore, a simple calculation for energies of three-level systems of $^4RT^0$, $^2RT^0$, and $^2CT^0$ states is carried out to estimate J value at the closet approach of the RT pair. In the beginning,

Zeemann and ZFS interactions are ignored and Hamiltonian is written by

$$\hat{H} = \hat{H}_{ex} + \hat{H}_{CT} \tag{12}$$

where H_{ex} is the exchange integral and H_{CT} is the intermolecular CT interaction. The spin wavefunctions of $^4RT^0$, $^2RT^0$, and $^2CT^0$ states are as follows:

$$|^4RT^0 \pm \tfrac{1}{2}\rangle = \sqrt{\tfrac{2}{3}}|0\rangle|\pm\tfrac{1}{2}\rangle + \tfrac{1}{\sqrt{3}}|\pm1\rangle|\mp\tfrac{1}{2}\rangle$$

$$|^4RT^0 \pm \tfrac{3}{2}\rangle = |\pm1\rangle|\pm\tfrac{1}{2}\rangle$$

$$|^2RT^0 \pm \tfrac{1}{2}\rangle = -\tfrac{1}{\sqrt{3}}|0\rangle|\pm\tfrac{1}{2}\rangle + \sqrt{\tfrac{2}{3}}|\pm1\rangle|\mp\tfrac{1}{2}\rangle$$

$$|^2CT^0 \pm \tfrac{1}{2}\rangle = |T^{1-}\pm\tfrac{1}{2}\rangle \tag{13}$$

These spin wave functions of the RT encounter complexes are expressed by using triplet ($|\pm1\rangle$ and $|0\rangle$) and doublet ($|\pm1/2\rangle$) basis sets for the triplet and the radical molecules, respectively, and the CT complex is described by $|T^{1-}\pm1/2\rangle$ for the anion radical formed by electron transfer from Galv to triplet molecule. The secular equation for $^4RT^0$, $^2RT^0$, and $^2CT^0$ states at the closest approach of the pair is then written as

$$\begin{vmatrix} -J_{ex}-E & 0 & 0 \\ 0 & J_{ex}-E & H_{CT} \\ 0 & H_{CT} & \Delta G - E \end{vmatrix} \begin{matrix} {}^4RT^0 \\ {}^2RT^0 \\ {}^2CT^0 \end{matrix} = 0. \tag{14}$$

We assume that CT interaction is not large enough to give remarkable effects on the electronic wave functions of the triplet and the radical molecules in RT encounter pairs and change in J_{ex} value due to CT-mediated mixing between $^2RT^0$ and $^2CT^0$ states is negligibly small. This may be reasonable because no exciplex formations are recognized in the excited molecule and Galv pairs studied here, which suggests that CT interaction is relatively small. Energy shift of $^2RT^0$ caused by the $^2CT^0$ state at the closest approach, defined as J_{CT}, is then calculated by a simple perturbation theory as

$$J_{CT} \cong -\frac{H_{CT}(d)^2}{\Delta G} \tag{15}$$

J_{ex} in the denominator was excluded because the exchange integral in the encounter pairs is around 1 cm^{-1} or much less, which is negligibly small compared to ΔG value unless the ΔG value of RT pairs of interest is nearly zero. The diagonalized secular equation is then written by

$$\begin{vmatrix} -J_{ex}-E & 0 & 0 \\ 0 & J_{ex}+J_{CT}-E & 0 \\ 0 & 0 & \Delta G - J_{CT} - E \end{vmatrix} = 0. \tag{16}$$

In the present study, we investigate RT systems with wide range of ΔG values including the systems with ΔG values of nearly zero. Simple perturbation theory cannot be applied to these systems of close degeneracies. In particular, the RT pairs of $\Delta G \approx 0$ is very interesting because the sign of J value changes around $\Delta G = 0$. Therefore, we solve the secular eq 14 for $\Delta G \approx 0$ systems by performing approximate calculations.

The characteristic feature in the present data is that λ_s(r) is negligibly smaller than λ_v. Under this condition, we applied

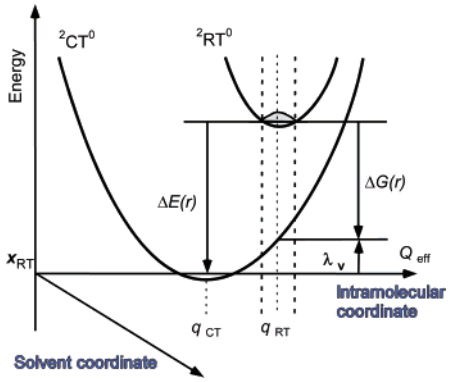

Figure 8. Schematic drawing of the potentials of RT and CT pairs.

treatment of Bixon et al.[23] for calculation of J value in radical ion pairs. In their model, the zero-order ion pair state is coupled to the background vibronic states of the counter-parted electronic states. Sum of the energy shifts of zero-order state caused by these vibronic states equals the J_{CT} value. A contribution of a certain vibronic state is calculated by multiplying a Franck−Condon weighted density, which is approximately described by symmetrical Gaussian shape. Their theory is for the radical ion pairs formed in the photosynthetic center in which solvent reorganization energy is neglected. In the present $^2CT^0$−$^2RT^0$ system in benzene, $\lambda_s(r)$ is negligibly small (0.02 eV) compared to λ_v (0.25 eV) and the treatment of Bixon et al. is applicable. Under this condition, $\Delta G(r)$ and $\Delta E(r)$ are described as shown in Figure 8. In this model, potentials of both $^2CT^0$ and $^2RT^0$ states are described as a function of one effective vibrational mode, Q_{eff} used as a representative of multimode system. J_{CT} is then given by the following equation of principal value integral,

$$J_{CT} = \frac{H_{CT}(d)^2}{\sqrt{2\pi\lambda_v h\omega_{eff}}} P \int_{-\infty}^{\infty} \frac{\exp\left\{-\dfrac{(E-\lambda_v)^2}{2\lambda_v h\omega_{eff}}\right\}}{\Delta E(d) - E} \mathrm{d}E \tag{17}$$

where ω_{eff} is vibrational frequency of Q_{eff} mode. Figure 9a shows plots of J_{CT} as a function of ΔG values calculated by eq 17. In this simulation, $H_{CT}(d) = 1$ cm^{-1} as an example and $\lambda_v = 0.25$ eV are used. Because we consider weak CT interaction, the small $H_{CT}(d)$ value was tentatively adopted for the simulation. The $h\omega_{eff}$ values of 500, 800, 1000, and 1400 cm^{-1} are used for these trial calculations. As seen in Figure 9a, J_{CT} tends to be positive for $\Delta G < 0$ and negative for $\Delta G > 0$ and the sign of J_{CT} changes at $\Delta G = 0$. As $h\omega_{eff}$ becomes larger, the plot indicates broader feature.

The Q−D energy difference in RT pair at the closest approach, J_0 is finally calculated by

$$J_0 = J_{ex} + J_{CT} \tag{18}$$

The exchange integral is described by the overlap integral of two molecules in the encounter complex, and thus we assume that this value is roughly constant for Galv/triplet systems studied here and is independent of ΔG. According to the CIDEP study, the sign of J value is negative in the regions of $\Delta G >$ 0 kJ mol^{-1} and $\Delta G < -40$ kJ mol^{-1}. A major component of J_0 value in the region of $\Delta G \ll -40$ kJ mol^{-1} cannot be J_{CT} because the sign of J_{CT} should be positive and $|J_{CT}|$ of the pair with large $|\Delta G|$ value is small according to eq 15. Therefore, we consider that J_{ex} dominates J_0 value in the region of $\Delta G \ll -40$ kJ mol^{-1}. The sign of J_{ex} should be negative for

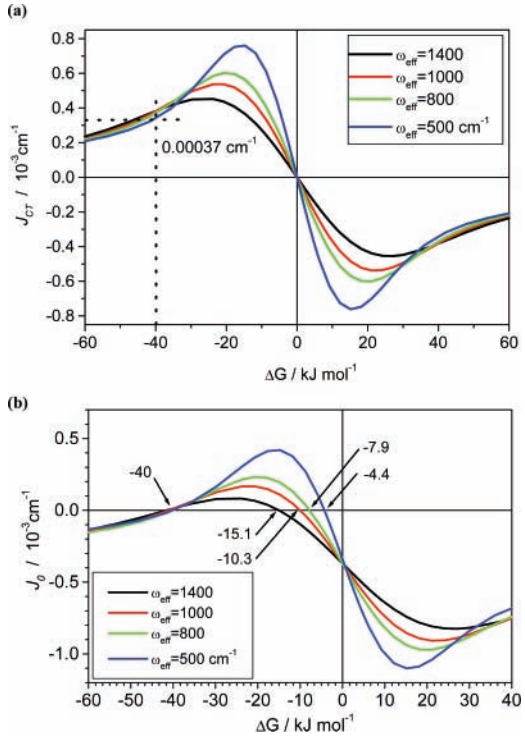

Figure 9. Theoretical calculation of J_{CT} and J_0 values as a function of ΔG values between RT and CT pair states. Numbers with arrows in (b) indicate the ΔG values for $J_0 = 0$. Details are explained in the text.

Galv/triplet systems because the usually encountered pair of paramagnetic species shows antiferromagnetic interaction.[5] The sign of P_n value changes around $\Delta G = -40$ kJ mol^{-1} region, as shown in Figure 7, and we consider that $|J_{ex}|$ equals to $|J_{CT}|$ for RT pairs of $\Delta G = -40$ kJ mol^{-1} where J_{CT} is $+0.00037$ cm^{-1} according to this trial calculation shown in Figure 9a. Therefore, we applied $J_{ex} = -0.00037$ cm^{-1} as the representative value of J_{ex} in Galv/triplet systems for the calculation of J_0 value by eq 16 when we assume the $H_{CT}(d) = 1$ cm^{-1} condition. According to this procedure for the calculation of J_0 value, we obtained theoretical curves for J_0 vs ΔG, as shown in Figure 9b. The sign of J_0 value is positive in $\Delta G = -40$ to -4.4 kJ mol^{-1} region with ω_{eff} of 500 cm^{-1}, while $\Delta G = -40$ to -15.1 kJ mol^{-1} region with ω_{eff} of 1400 cm^{-1}. According to the CIDEP results, the sign of the P_n value, i.e., the sign of J_0, changes around $\Delta G = 0$ as well as -40 kJ mol^{-1}. Among the J_0 curves for various ω_{eff} values, the curve with ω_{eff} of 500 cm^{-1} shows the better agreement with the experimentally determined sign of the P_n value. The calculated curves with $\omega_{eff} < 500$ cm^{-1} are essentially the same as that of $\omega_{eff} = 500$ cm^{-1}, namely, the sign of J_0 value changes when ΔG nearly equals 0. Therefore, we use the J_0 curves with $\omega_{eff} = 500$ cm^{-1} in the following discussion.

***P_n* Values Calculated by Shushin's Diffusion Theory for CIDEP Created by RTPM.** The last step of the present theoretical analysis for the experimetal results is to calculate P_n according to the diffusion theory for CIDEP creation[19,20] with a theoretically calculated J_0 value. For calculation of P_n values by the CIDEP theory, the exchange interaction, $J(r)$, for $^{2,4}RT^0$ states is important. In usual approximation, the exchange interaction is given by the exchange integral, which decays exponentially as r becomes larger. Thus, $J_{ex}(r)$ is expressed by the equation.[20]

$$J_{ex}(r) \cong -J_{ex} \exp\{-\gamma_{ex}(r-d)\} \tag{19}$$

Similarly, CT interaction approximately depends on the overlap integral of the molecular orbitals of the pair and is expressed by another exponentially decaying function as,

$$J_{CT}(r) \cong -J_{CT} \exp\{-\gamma_{CT}(r-d)\} \tag{20}$$

Because γ_{ex} and γ_{CT} are both parameters related to the overlap integral of the pair molecules, we assume that these values are identical. Under this approximation, the $J(r)$ value is derived by eq 18 and expressed by the formula

$$J(r) = -(J_{ex} + J_{CT}) \exp\{-\gamma(r-d)\} \tag{21}$$

There is a possibility that γ_{ex} is largely different from γ_{CT}. In such a case, $J(r)$ is not expressed by the exponentially decaying function, and it is quite interesting that the sign of the $J(r)$ value could depend on the intermolecular distance when J_{ex} and J_{CT} are in opposite signs. Recent experimental findings indicate such a possibility.[37] Although this interesting feature is worthwhile to discuss, we confine ourselves in this study to the model with the usual exponentially decaying function assuming γ_{ex} and γ_{CT} are essentially same and expressed by γ.

The Hamiltonian for the present spin system under a magnetic field is

$$\begin{aligned}\hat{H}(r) &= \hat{H}_{Zeeman} + \hat{H}_{ex} + \hat{H}_{ZFS} \\ &= g\beta B(\hat{S}_{Tz} + \hat{S}_{Rz}) - \frac{1}{3}J(r)(1 + 4\hat{S}_T\hat{S}_R) + \\ &\qquad D_{ZFS}\left(\hat{S}^2_{T\zeta} - \frac{1}{3}\hat{S}^2_T\right)\end{aligned} \tag{22}$$

where symbols are in their usual meanings and E_{ZFS} parameter in ZFS interaction is neglected because $E_{ZFS} \ll D_{ZFS}$ for usual triplet states of organic compounds.[30,32] Here, we applied Shushin's diffusion theory for CIDEP magnitude due to the RTPM.[20] Shushin derived the formula for P_n value by solving the stochastic−Liouville equation including diffusion term and the spin relaxation superoperator for the RT pair. The spin polarization, P_n is expressed as a function of $J_0(= -J_{ex} - J_{CT})$ by the following equation

$$P_n = \frac{d^2\tau_c}{2D_r\gamma r_i}\sum\overline{|\langle Qm|H_{zfs}|Dm'\rangle|^2}F(\omega_{mm'},J_0) \tag{23}$$

where τ_c is the correlation time, D_r is the diffusion constant in the solvent, and r_i is the RT distance where the triplet quenching event occurs. In the present RT systems, it is assumed that r_i equals to d because the quenching rate constants are slightly smaller than the diffusion rate constant and the contact of RT pair is necessary for the quenching. The m and m' are the spin states of Q and D, respectively, and $\omega_{mm'}$ is the Zeeman energy difference between m and m' states. The function $F(\omega,J_0)$ in eq 23 is given by the following formula.

$$\begin{aligned}F(\omega,J_0) &= \frac{y}{1+y^2}\int_0^\infty \left(\frac{1}{1+[\omega + 2J_0\exp(-r)]^2\tau_c^2} - \right. \\ &\qquad \left. \frac{1}{1+[\omega - 2J_0\exp(-r)]^2\tau_c^2}\right)dr \\ &= \frac{y}{1+y^2}\left[\{\arctan(u_-) - \arctan(u_+)\} + \right. \\ &\qquad \left. \frac{y}{2}\ln\left(\frac{1+u_-^2}{1+u_+^2}\right)\right]\end{aligned} \tag{24}$$

where

$$u_{\pm} = (\omega \pm 2J_0)\tau_c, \text{ and } y = \frac{1}{\omega\tau_c} \qquad (25)$$

From these equations and J_0 values obtained by the analysis in Figure 9, P_n values can be calculated as a function of ΔG value.

In the calculation for P_n values by eq 23, we assume a simple model RT system with unique values of D_{ZFS}, D_r, and τ_c. We used the following parameters: Zeeman energy for a half spin, $\omega_0 = g\beta B_0 = 6.0 \times 10^{10}$ rad·s^{-1} under the X-band EPR measurements, and D_{ZFS} value[30,32] of 1.8×10^{10} rad·s^{-1} for usual organic triplet molecules of one or two ring sizes. The diffusion coefficient of 1.4×10^{-5} cm^2·s^{-1} was used for Galv and triplet molecules because reported diffusion constants of some organic compounds are $1.2-1.5 \times 10^{-5}$ cm^2·s^{-1} in benzene or in cyclohexane at room temperature,[38] which may be good representative D_r values of organic compounds studied here. Therefore, $D_r = 2.8 \times 10^{-5}$ cm^2·s^{-1}, which corresponds to the sum of D_r values of Galv and triplet molecules, was used for Galv/triplet systems. The τ_c was estimated to be 28 ps from the Debye equation for rotational correlation time with $\eta = 0.649$ mPa·s and molecular radius of 0.35 nm.[29] The parameters in $J(r)$ of Galv/triplet pair were assumed to be on the same order of the magnitude with those in the collisional radical pairs and RT pairs. Thus, we used $d = 0.7$ nm and γ values on the order of nm^{-1}. For J_0 value, we adopted calculated results based on Bixon's model with $\omega_{eff} = 500$ cm^{-1}.

The magnitude of J_0 may change largely as a function of ΔG and it should contribute to P_n. Therefore, P_n values as a function of $H_{CT}(d)$, which controls J_0 value, were calculated with the constant γ value of 8 nm^{-1}, as shown in the plots of Figure 10a. The γ of 8 nm^{-1} was reported for γ value in the triplet benzophenone/nitroxyl pair based on CIDEP analysis,[13] and we consider that this may be a good representative value for the RT pair model. For the plots of each $H_{CT}(d)$ value, the magnitude of J_{ex} values were adjusted to satisfy the condition $J_{ex} = -J_{CT}$ at $\Delta G = -40$ kJ·mol^{-1}. The ΔG dependence of P_n value in Figure 9a drastically changes as a function of $H_{CT}(d)$ value. For low $H_{CT}(d)$ (<10 cm^{-1}), $|J_0|$ is smaller than ω_0, which is called the weak exchange limit[20] and P_n value changes rather gradually. For high $H_{CT}(d)$ (>30 cm^{-1}), $|J_0|$ is larger than ω_0, which is called the strong exchange limit,[20] and the P_n value changes drastically around the region where J_0 changes its sign. In the latter case, it is clear from the Figure 10a that P_n value is either $+6\,P_{eq}$ for $J_0 > 0$ or $-6\,P_{eq}$ for $J_0 < 0$. Any larger J_0 values satisfying $|J_0| > \omega_0$ lead essentially to the same results, and better agreement with experimentally determined P_n value was obtained. On the other hand, $H_{CT}(d)$ of less than 10 cm^{-1} giving small $|J_0|$ value does not show a good consistence with the experimental results on P_n values. Therefore, we conclude that any $H_{CT}(d)$ values larger than 30 cm^{-1} can reproduce the feature of ΔG dependent experimental P_n values. In the studies of electron-transfer reactions between aromatic compounds, $H_{CT}(d)$ values at the contact distance is on the order of 10 cm^{-1} or more.[39] It may be reasonable that $H_{CT}(d)$ of Galv/triplet pairs is larger than 30 cm^{-1}. For instance, $H_{CT}(d) = 60$ cm^{-1} gives J_{CT} of 1.3 cm^{-1} at $\Delta G = -40$ kJ mol^{-1}, and the corresponding J_{ex} value is -1.3 cm^{-1}, which is ca. 4 times larger than Zeeman energy. This energy relation indicates that the RT pair belongs to a strong exchange limit case. This feature is in good consistence with the previous studies on J_{ex} value in RT encounter pairs such as nitroxide/triplet, benzil ketyl/triplet, and α,γ-bisdiphenylene-β-phenylallyl/triplet systems.[13−15,17] Next we examine the γ value for ΔG dependence of P_n value. Figure 10b shows some examples of calculated P_n values for various γ values of 3−20 nm^{-1}. In this calculation, $H_{CT}(d)$ of 60 cm^{-1} was taken as a rough guide of the value. The maximum and the minimum P_n values largely depend on the γ value. According to the analysis in the plots, $\gamma = 8-12$ nm^{-1} gives better agreement with the experimental P_n values. The parameters determined by the present analysis are summarized in Table 2, together with the literature values of CT interaction parameters in radical ion pairs derived from the analysis on electron-transfer kinetics. The $H_{CT}(d)$ values greater than 30 cm^{-1} for Galv/triplet pairs seem reasonable as compared with the values in radical ion pairs.

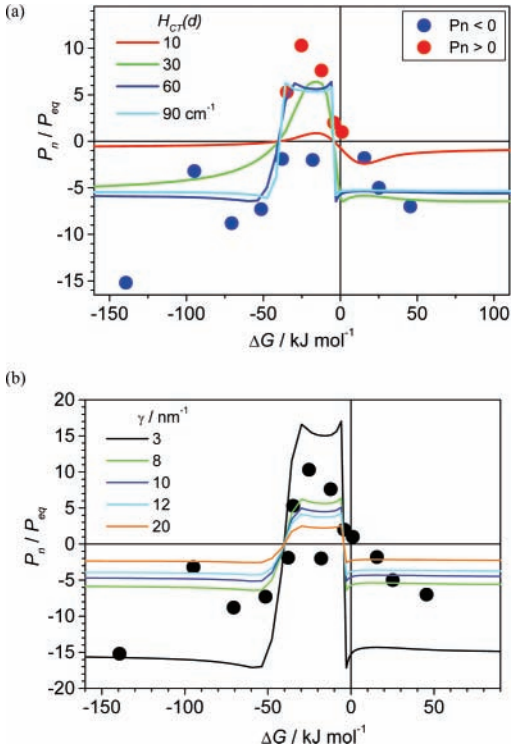

Figure 10. Solid lines are ΔG dependent theoretical P_n values calculated by diffusional theory for CIDEP in the RTPM. Dependence on (a) $H_{CT}(d)$ with $\gamma = 8$ nm^{-1} and (b) γ values with $H_{CT}(d) = 60$ cm^{-1}. Details are explained in the text.

Nature of *J* Value in Radical-Triplet (RT) Pairs. It might be interesting to consider the reason why the CT interaction is dominant in Galv/triplet pairs and to discuss a nature of J value in RT pairs. As pointed out previously, the sign of J value in the radical ion pairs is totally controlled by CT effect. This is in accord with the fact that the radical ion pairs of organic compounds do not form stable chemical bonds, namely, exchange integrals between the cation and anion radicals are generally small. This situation in radical ion pairs is quite different from the case in RT pairs, where a balance between exchange integrals and CT effects is definitely important in the sign inversion of J value. So far, we have studied the sign of J value intensively for the RT pairs, TEMPO or Galv radical with various kinds of triplet molecules. It turns out that all the RT pairs of TEMPO examined show negative sign of J value. On the other hand, several Galv/triplet pairs have been found to show positive J values because the CT effect is dominant in these pairs as discussed in this study. To understand this interesting experimental finding on the radical-dependent nature of the sign inversion of J value, we carried out the J_{CT} estimation by introducing the appropriate values of parameters ($H_{CT}(d)$, λ_v, and ω_{eff}) into eq 17 as well as examination of J_{ex} value.

TABLE 2: Parameters of CT Interaction and Intermolecular Potential of Galv/triplet Encounter Pairs Used for the Analysis of P_n Vs ΔG Plots, Together with the Parameters Reported for Encounter Radical Ion Pairs.

pair type	pair species[a]	$H_{CT}(d)$/cm^{-1}	ω_{eff}/cm^{-1}	λ_v/kJ mol^{-1}	γ/nm^{-1}
contact radical-triplet pairs	galv radical /triplet (see Table 1)[b]	>30	<500	24	8∼12
solvent separated radical ion pairs	cation (DCA or TCA)/anion (Np, Bip, Phen, or Bz)[c]	8.0∼11.5	1400∼1500	19.3∼24	
contact radical ion pairs	TCA cation/Bz anion[d]	700∼1300	1400	19.3	

[a] DCA: 9,10-dicyanoanthracene; TCA: 2,6,9,10-tetrachyanoanthracene; Np: alkylnaphthalene derivatives; Bip: alkylbiphenyl derivatives; Phen: alkylphenol derivatives; Bz: alkylbenzene derivatives. [b] This work. [c] Taken from refs 34 and 39d. [d] Taken from ref 34.

Among parameters in eq 17, λ_v value can be roughly estimated by a quantum chemical calculation. To evaluate a difference in λ_v value of RT pairs between Galv and TEMPO, we consider λ_v value as being divided into two parts, which are λ_v values for the radical (λ_v^r) and the triplet (λ_v^T). For λ_v^r, we calculated electronic energies of Galv cation (Galv$^+$) at two different structures, which are the optimized structures of Galv radical and Galv$^+$ cation. The difference between these two energies corresponds to λ_v^r value. A similar calculation was carried out for the TEMPO radical. According to the calculations at the B3LYP/6-31G(d) level of theory,[40] we found that λ_v^r value is quite different depending on radicals, 8.5 kJ mol^{-1} for Galv radical and 48.0 kJ mol^{-1} for TEMPO radical. The λ_v^r values are related to the structural changes from Galv to Galv$^+$ and from TEMPO to TEMPO$^+$. The large difference in λ_v^r value is important because the Franck−Condon factor between radical and radical$^+$ is remarkably different between TEMPO and Galv. Larger λ_v^r value of TEMPO indicates the significant structural change from TEMPO to TEMPO$^+$. In eq 17, a fluctuation of J_{CT} value due to vibration motion along the coordinate of the effective mode was considered and averaged J_{CT} value was calculated assuming the Gaussian shape of the wave function for Q_{eff} mode. In this calculation, continuum background states in CT pairs are assumed to exist.[23] If the structural change from RT to CT states is significant, the Franck−Condon factor between the two states is expected to be small. Our quantum chemical calculation suggests the significant structural change from TEMPO to TEMPO$^+$, which means that the Franck−Condon factor for TEMPO/triplet pairs is much smaller than that for Galv/triplet pairs. Therefore, we expect that the J_{CT} value is larger in Galv/triplet pairs than the value in TEMPO/triplet pairs.

The $H_{CT}(d)$ and J_{ex}, which are the other important factors to control J value, are in proportion to the overlap integral between radical and triplet molecule. The SOMO of TEMPO is rather localized in the NO group, while Galv has a diffuse SOMO delocalized over the two phenyl type groups. The overlap integral of RT pairs is thus expected to be larger in the TEMPO/triplet pair than in the Galv/triplet pair. This means that both the $H_{CT}(d)$ and J_{ex} values would be larger in TEMPO than in Galv. According to this estimation limited to $H_{CT}(d)$ and J_{ex} values, both J_{CT} and J_{ex} will be larger in TEMPO/triplet pair. To explain the sign of J value, we should tell which factor of J_{CT} and J_{ex} is more dominant in RT pairs. Therefore, a simple comparison of $H_{CT}(d)$ to J_{ex} will not give us the reason why J_{CT} value is significant in Galv/triplet pairs but not in TEMPO/triplet pairs. The larger ω_{eff} value corresponds to the larger $|J_{CT}|$ value for a certain ΔG value near the $\Delta G = 0$ region as shown in Figure 9. This ω_{eff} parameter requires experimental results such as plots in Figure 7 to be determined. Unfortunately, we do not have data on P_n values vs ΔG in TEMPO/triplet pairs. No clear theoretical explanation is found for the proper value of ω_{eff}, which is necessary to explain interaction between RT and CT pair states. At this moment, we are not able to discuss our results based on ω_{eff} value.

Consequently, we consider that J value of TEMPO/triplet pairs is controlled mostly by J_{ex}, presumably with a small contribution from J_{CT}. Because J_{ex} is generally negative in sign, J value of TEMPO/triplet pair shows negative sign. Meanwhile, J value of Galv/triplet pair is more dominantly controlled by J_{CT} owing to similar structures of RT and CT pair states, which results in positive J value for some RT pairs with ΔG being negative and close to zero. Our experimental finding on the nature of J value is reasonably explained by a CT-controlled exchange interaction examined in the present study.

It is noteworthy that the P_n value for Galv/TPP (tetraphenylporphin) pair shows an exceptional negative sign although the estimated ΔG of −17.9 kJ mol^{-1} may indicate the positive J value (see Table 1 and Figure 10). Actually, the P_n values of the other Galv/triplet pairs in the ΔG range of −40 to 0 kJ mol^{-1} are positive in sign. We consider the plausible reasons below. (1) The size of TPP is remarkably large among the molecules studied in this work, and the estimation of λ_v value of the Galv/TPP pair might be much larger than 24.0 kJ mol^{-1} used for the present energy calculation. It was pointed out by Gould et al. that the λ_v values of the aromatic compounds become larger as the number of the ring increases.[34] If the λ_v value becomes twice as large as the other aromatic molecules, the ΔG value for the Galv/TPP pair becomes positive and the negative sign of P_n value might be explained reasonably. However, a quantum chemical calculation for the λ_v^T value of TPP performed by the similar procedure as described for the λ_v^r calculation gives 10.3 kJ mol^{-1}, which is not beyond our approximation using $\lambda_v = 24.0$ kJ mol^{-1} for Galv/triplet pairs. (2) Porphyrin derivatives such as TPP are rather unique molecules as compared to the other molecules studied here because their rotational motion is remarkably slow and even the TR-EPR signal of their triplet can be detected in the solution at room temperature.[4b,41] In this study, we assume that the rotation correlation time is fast enough to average out the fluctuating J value due to anisotropic interaction between the two molecules of RT pairs. However, slow rotation of TPP may provide anisotropic effects on J value. Although the detailed mechanism to give negative J value is still unknown, we suppose that the sign of J value is related to some anisotropic effect on the Galv/TPP pair interaction.

Concluding Remarks

As a conclusion for the present study on Galv/triplet pairs, experimental results of P_n values as a function of ΔG are reasonably explained by a theoretical analysis of Shushin's diffusion theory for RT pairs, with their J_0 values controlled by both exchange integral of $^{2,4}RT^0$ states and intermolecular CT interactions between $^2RT^0$ and $^2CT^0$ states. When exchange integral dominates J_0 value, the sign of J_0 is negative. On the other hand, when intermolecular CT interaction dominates, J_0 value becomes positive for $\Delta G < 0$. The ΔG range of −40−0 kJ mol^{-1} for positive J_0 value was well reproduced by Bixon's model for intermolecular CT interaction with nearly degenerate systems of RT and CT pair states.

For more complete understanding of J value in RT pairs, we have to examine values appearing in eq 17 such as $H_{CT}(d)$ and ω_{eff} as well as Franck−Condon factors. To perform this investigation, we should expand our target to other RT pairs such as TEMPO/triplet and DPPH/triplet pairs. For these pairs, it is necessary to show clear evidence that the RT pairs have some effects due to CT controlled exchange interaction through detailed studies on P_n vs ΔG, as demonstrated in this study for Galv/triplet pairs. These will be a future plan to understand the nature of RT encounter complexes.

Acknowledgment. This work was supported in part by a Grant-in-Aid for Scientific Research (nos. 17350005 and 15550005) from the Ministry of Education, Science, Culture and Sports of Japan. This study was performed using one of on-campus cooperative research facilities in Tokyo Institute of Technology, "a pulsed ESR system".

Supporting Information Available: Schematic diagram of sapphire dielectric resonator and an excitation laser beam trajectory. This material is available free of charge via the Internet at http://pubs.acs.org.

References and Notes

(1) (a) Nagakura, S., Hayashi, H., Azumi, T., Eds. *Dynamic Spin Chemistry*; Kodansha: Tokyo; Wiley & Sons: New York, 1998. Steiner, U. E.; *Chem. Rev.* **1989**, *89*, 51. (b) Molin, Yu. N. *Spin Polarization and Magnetic Effects in Radical Reactions*; Elsevier: New York, 1984. Muus, L. T.; Atkins, P. W.; McLauchlan, K. A.; Pedersen, J. B. *Chemically Induced Magnetic Polarization*; D. Reidel Publishing Company: Dordrecht, The Netherlands, 1977. Adrian, F. J. *Res. Chem. Intermed.* **1979**, *3*, 3. (c) van-Willigen, H. *Chem. Rev.* **1993**, *93*, 173.

(2) (a) Gijzeman, O. L. J.; Kaufman, F.; Porter, G. *J. Chem. Soc., Faraday Trans. 2* **1973**, *69*, 727. (b) Razi.Naqvi, K. *J. Phys. Chem.* **1981**, *85*, 2303. (c) Watkins, A. R. *Chem. Phys. Lett.* **1980**, *70*, 262. (d) Kuzumin, V. A.; Klinger, D. S.; Hammond, G. S. *Photochem. Photobiol.* **1980**, *31*, 607. (e) Hiratsuka, H.; Rajadurai, S.; Das, P. K.; Hug, G. L.; Fessenden, R. W. *Chem. Phys. Lett.* **1987**, *137*, 255.

(3) (a) Chattopadhyay, S. K.; Das, P. K.; Hug, G. L. *J. Am. Chem. Soc.* **1983**, *105*, 6205. (b) Suzuki, T.; Obi, K. *Chem. Phys. Lett*. **1995**, *246*, 130.

(4) (a) Imamura, T.; Onitsuka, O.; Obi, K. *J. Phys. Chem.* **1986**, *90*, 6741. (b) Fujisawa, J.; Ishii, K.; Ohba, Y.; Iwaizumi, Y.; Yamauchi, S. *J. Phys. Chem.* **1995**, *99*, 17082.

(5) (a) Blättler, C.; Jent, F.; Paul, H. *Chem. Phys. Lett.* **1990**, *166*, 375. (b) Kawai, A.; Okutsu, T.; Obi, K. *J. Phys. Chem.* **1991**, *95*, 9130. (c) Kawai, A.; Obi, K. *J. Phys. Chem.* **1992**, *96*, 52. (d) Kawai, A.; Obi, K. *J. Phys. Chem.* **1992**, *96*, 5701. (e) Kawai, A.; Obi, K. *Res. Chem. Intermed.* **1993**, *19*, 866. (f) Kawai, A. *Appl. Magn. Reson.* **2003**, *23*, 349. (g) Kawai, A.; Shiubya, K. *J. Photochem. Photobiol., C* **2006**, *7*, 89.

(6) (a) Turro, N. J.; Khudyakov, I. V.; Dwyer, D. W. *J. Phys. Chem.* **1993**, *79*, 10530. (b) Khudyakov, I. V.; Turro, N. J. *Res. Chem. Intermed.* **1993**, *19*, 15.

(7) (a) Kobori, Y.; Kawai, A.; Obi, K. *J. Phys. Chem.* **1994**, *98*, 6425. (b) Mitsui, M.; Takeda, K.; Kobori, Y.; Kawai, A.; Obi, K. *Chem. Phys. Lett.* **1996**, *262*, 125.

(8) (a) Corvaja, C.; Maggini, M.; Prato, M.; Scorrano, G.; Venzin, M. *J. Am. Chem. Soc*. **1995**, *117*, 8857. (b) Teki, Y.; Miyamoto, S.; Nakatsuji, M.; Miura, Y. *J. Am. Chem. Soc.* **2001**, *123*, 294. (c) Ballesteros, O. G.; Maretti, L.; Sastre, R.; Scaiano, J. C. *Macromolecules* **2001**, *34*, 6184. (d) Sartori, E.; Toffoletti, A.; Rastrelli, F.; Corvaja, C.; Bettio, A.; Formaggio, F.; Oancea, S.; Toniolo, C. *J. Phys. Chem. A* **2003**, *107*, 6905. (e) Franco, L.; Mazzoni, M.; Corvaja, C.; Gubskaya, V. P.; Berezhnaya, L. Sh.; Nuretdinov, I. A. *Mol. Phys.* **2006**, *104*, 1543.

(9) (a) Ishii, K.; Fujisawa, J.; Ohba, Y.; Yamauchi, S. *J. Am. Chem. Soc*. **1996**, *118*, 13079. (b) Fujisawa, J.; Ishii, K.; Ohba, Y.; Yamauchi, S.; Fuhs, M.; Möbius, K. *J. Phys. Chem. A* **1997**, *101*, 5869. (c) Maretti, L.; Saiful, Islam, S. M.; Kajiwara, T.; Miyamoto, R.; Ohba, Y.; Yamauchi, S. *Mol. Phys.* **2006**, *104*, 1619.

(10) (a) Michaeli, S.; Meiklyar, V.; Schulz, M.; Moebius, K.; Levanon, H. *J. Phys. Chem.* **1994**, *98*, 7444. (b) Asano-Someda, M.; van der Est, A.; Krgüer, U.; Stehlik, D.; Kaizu, Y.; Levanon, H. *J. Phys. Chem. A* **1999**, *103*, 6704. (c) Kandrashkin, Y. E.; Asano-Someda, M.; van der Est, A. *J. Phys. Chem. A* **2006**, *110*, 9617. (d) Asano-Someda, M.; Ishizuka, K.; Kaizu, Y. *Mol. Phys.* **2006**, *104*, 1609.

(11) (a) Mori, Y.; Sakaguchi, Y.; Hayashi, H. *J. Phys. Chem. A* **2002**, *106*, 4453. (b) Ivanov, K. L. *J. Phys. Chem. A* **2005**, *109*, 5160. (c) Mi, Q.; Chernick, E. T.; McCamant, D. W.; Weiss, E. A.; Ratner, M. A.; Wasielewski, M. R. *J. Phys. Chem. A* **2006**, *110*, 7323.

(12) Poole, C. P., Jr.; Frach, H. A. *Handbook of Electron Spin Resonance*; American Institute of Physics: Woodbury, NY, 1994.

(13) (a) Goudsmit, G. H.; Paul, H.; Shushin, A. I. *J. Phys. Chem.* **1993**, *97*, 19243. (b) Goudsmit, G. H.; Paul, H.; *Chem. Phys. Lett.* **1993**, *208*, 73. (c) Blättler, C.; Paul, H. *Res. Chem. Intermed.* **1991**, *16*, 201.

(14) (a) Kobori, Y.; Takeda, K.; Tsuji, K.; Kawai, A.; Obi, K. *J. Phys. Chem. A* **1998**, *102*, 5160. (b) Kobori, Y.; Mitsui, M.; Kawai, A.; Obi, K. *Chem. Phys. Lett.* **1996**, *252*, 355.

(15) (a) Terazono, H.; Kawai, A.; Tsuji, K.; Shibuya, K. *J. Photochem. Photobiol., A* **2006**, *183*, 22. (b) Mitsui, M.; Takeda, K.; Kobori, Y.; Kawai, A.; Obi, K. *J. Phys. Chem. A* **2004**, *108*, 1120. (c) Mitsui, M.; Kobori, Y.; Kawai, A.; Obi, K. *J. Phys. Chem. A* **2004**, *108*, 524.

(16) Turro, N. J.; Koptyug, I. V.; Willingen, H. V.; McLauchlan, K. A. *J. Magn. Reson., Ser. A* **1994**, *109*, 121.

(17) (a) Blank, A.; Levanon, H. *J. Phys. Chem. A* **2000**, *104*, 794. (b) Blank, A.; Levanon, H. *J. Phys. Chem. A* **2001**, *105*, 4799.

(18) (a) Martínez, C. G.; Jockusch, S.; Ruzzi, M.; Sartori, E.; Moscatelli, A.; Turro, N. J.; Buchachenko, A. L. *J. Phys. Chem. A* **2005**, *109*, 10216. (b) Stavitski, E.; Wagnert, L.; Levanon, H. *J. Phys. Chem. A* **2005**, *109*, 976.

(19) Shushin, A. I. *Z. Phys. Chem.* **1993**, *182*, 9.

(20) (a) Shushin, A. I. *Chem. Phys. Lett.* **1993**, *208*, 173. (b) Shushin, A. I. *Chem. Phys. Lett.* **1999**, *313*, 246. (c) Shushin, A. I. *Mol. Phys.* **2002**, *100*, 1303.

(21) Adrian, F. J. *Chem. Phys. Lett.* **1994**, *229*, 465.

(22) Andersen, P. W. *Phys. Rev.* **1959**, *115*, 2.

(23) Bixon, M.; Jortner, J.; Michel-Beyerle, M. E. *Z. Phys. Chem.* **1993**, *180*, 193.

(24) (a) Sekiguchi, S.; Kobori, Y.; Akiyama, K.; Tero-Kubota, S. *J. Am. Chem. Soc.* **1998**, *120*, 1325. (b) Kobori, Y.; Sekiguchi, S.; Akiyama, K.; Tero-Kubota, S. *J. Phys. Chem. A* **1999**, *103*, 5416. (c) Kobori, Y.; Akiyama, K.; Tero-Kubota, S. *J. Chem. Phys.* **2000**, *113*, 465.

(25) Kawai, A.; Shibuya, K.; Obi, K. *Appl. Magn. Reson.* **2000**, *18*, 343.

(26) (a) Kawai, A.; Watanabe, Y.; Shibuya, K. *Mol. Phys.* **2002**, *100*, 1225. (b) Kawai, A.; Watanabe, Y.; Shibuya, K. *Chem. Phys. Lett.* **2003**, *372*, 8. (c) Rozenshtein, V.; Berg, A.; Stavitski, E.; Levanon, H.; Franco, L.; Corvaja, C. *J. Phys. Chem. A* **2005**, *109*, 11144.

(27) Kawai, A.; Shibuya, K. *J. Phys. Chem. A* **2002**, *106*, 12305.

(28) Verma, N. C.; Fessenden, R. W. *J. Chem. Phys.* **1976**, *65*, 2139.

(29) Atherton N. M. *Principles of Electro Spin Resonance*; Prentice Hall: New York, 1993.

(30) Murov, S. L.; Carmichael I.; Hug G. L. *Handbook of Photochemistry*; Marcel Dekker: New York, 1993.

(31) Yekta, A.; Turro, N. J. *Mol. Photochem.* **1972**, *3*, 307.

(32) Scaiano, J. C. *Handbook of Organic Photochemistry*; CRC Press: Boca Raton, FL, 1989; Vol. 2.

(33) Marcus, R. A. *J. Chem. Phys.* **1956**, *24*, 966.

(34) Gould, I. R.; Deniz, E.; Moser, J. E.; Farid, S. *J. Am. Chem. Soc.* **1990**, *112*, 4290.

(35) Samanta, A.; Bhattacharyya, K.; Das, P. K.; Kamat, P. V.; Weir, D.; Hug, G. L. *J. Phys. Chem.* **1989**, *3*, 3651.

(36) Chen, J. M.; Ho, T.-I.; Mon, C.-Y. *J. Phys. Chem.* **1990**, *94*, 2889.

(37) Kawai, A. *Appl. Magn. Reson.* **2004**, *26*, 213.

(38) (a) Okamoto, K.; Nogami, Y.; Tominaga, T.; Terazima, M. *Chem. Phys. Lett.* **2003**, *372*, 419. (b) Terazima, M.; Nogami, Y.; Tominaga, T. *Chem. Phys. Lett.* **2000**, *332*, 503. (c) Ukai, A.; Hirota, N.; Terazima, M. *Chem. Phys. Lett.* **2000**, *319*, 427. (d) Donkers, R. L.; Leaist, D. G. *J. Phys. Chem. B* **1997**, *101*, 304.

(39) (a) Miller, J. R.; Beitz, J. V.; Huddleston, R. K. *J. Am. Chem. Soc.* **1984**, *106*, 5057. (b) Miller, J. R.; Beitz, J. V. *J. Chem. Phys.* **1981**, *74*, 6476. (c) Miller, J. R.; Beitz, J. V. *J. Chem. Phys.* **1979**, *71*, 4579. (d) Gould, I. R.; Young, R. H.; Moody, R. E.; Farid, S. *J. Phys. Chem.* **1991**, *95*, 2068. (e) Weiss, E. A.; Ratner, M. A.; Wasielewski, M. R. *J. Phys. Chem. A* **2003**, *107*, 3639.

(40) Frisch, M. J.; Trucks, G. W.; Schlegel, H. B.; Scuseria, G. E.; Robb, M. A.; Cheeseman, J. R.; Montgomery, J. A., Jr.; Vreven, T.; Kudin, K. N.; Burant, J. C.; Millam, J. M.; Iyengar, S. S.; Tomasi, J.; Barone, V.; Mennucci, B.; Cossi, M.; Scalmani, G.; Rega, N.; Petersson, G. A.; Nakatsuji, H.; Hada, M.; Ehara, M.; Toyota, K.; Fukuda, R.; Hasegawa, J.; Ishida, M.; Nakajima, T.; Honda, Y.; Kitao, O.; Nakai, H.; Klene, M.; Li,

X.; Knox, J. E.; Hratchian, H. P.; Cross, J. B.; Bakken, V.; Adamo, C.; Jaramillo, J.; Gomperts, R.; Stratmann, R. E.; Yazyev, O.; Austin, A. J.; Cammi, R.; Pomelli, C.; Ochterski, J. W.; Ayala, P. Y.; Morokuma, K.; Voth, G. A.; Salvador, P.; Dannenberg, J. J.; Zakrzewski, V. G.; Dapprich, S.; Daniels, A. D.; Strain, M. C.; Farkas, O.; Malick, D. K.; Rabuck, A. D.; Raghavachari, K.; Foresman, J. B.; Ortiz, J. V.; Cui, Q.; Baboul, A. G.; Clifford, S.; Cioslowski, J.; Stefanov, B. B.; Liu, G.; Liashenko, A.; Piskorz, P.; Komaromi, I.; Martin, R. L.; Fox, D. J.; Keith, T.; Al-Laham, M. A.; Peng, C. Y.; Nanayakkara, A.; Challacombe, M.; Gill, P. M. W.; Johnson, B.; Chen, W.; Wong, M. W.; Gonzalez, C.; Pople, J. A. *Gaussian 03*, revision C.02; Gaussian, Inc.: Wallingford, CT, 2004.

(41) (a) Fujisawa, J.; Ohba, Y.; Yamauchi, S. *J. Phys. Chem. A* **1997**, *101*, 434. (b) Yamauchi, S.; Takahashi, A.; Iwasaki, Y.; Unno, M.; Ohba, Y.; Higuchi, J.; Blank, A.; Levanon, H. *J. Phys. Chem. A* **2003**, *107*, 1478. (c) Kawai, A.; Hidemori, T.; Shibuya, K. *Mol. Phys.* **2006**, *104*, 1573.